arXiv:1403.4570v2 [cond-mat.stat-mech] 19 Mar 2014

Dynamical phase transition induced order parameter oscillations in the nonequilibrium dynamics of the XXZ chain

M. Heyl
Institute for Quantum Optics and Quantum Information of the Austrian Academy of Sciences, 6020 Innsbruck, Austria and Institute for Theoretical Physics, University of Innsbruck, 6020 Innsbruck, Austria

In this work it is shown that the dynamics of the staggered magnetization in the XXZ chain after quantum quenches from initial Neél states is controlled by dynamical quantum phase transitions in Loschmidt echos. A direct connection between Loschmidt echos and the order parameter dynamics is established which links nonequilibrium microscopic probabilities to the system's macroscopic dynamical properties. These concepts are illustrated numerically using exact diagonalization. An outlook is given how to generalize these findings to other observables and to other systems with symmetry-broken phases.

Introduction:- In equilibrium thermodynamic phase transitions are accompanied by nonanalyticities in thermodynamic potentials leading to abrupt changes in the macroscopic physical properties. Out of equilibrium the real-time evolution in quantum many-body systems provides evidence for a dynamical analogue, a dynamical (phase) transition: the relaxational dynamics of observables can exhibit abrupt changes by varying external control parameters suggesting the possibility of different dynamical phases[1–15]. While the observed phenomenology is to a large extend compatible with a dynamical analogue the underlying principles are unclear and a framework allowing to address fundamental questions such as universality or robustness on general grounds is missing.

Systems which in equilibrium host a $\mathbb{Z}_2$-symmetry broken phase constitute one particular subclass of the above anticipated models in which the possibility of dynamical phase transitions has been suggested[3,11,12,14,15]. This is due to a generic feature observed in the nonequilibrium dynamics whenever the system is initially prepared in the symmetry-broken phase of the model. In consequence of a sudden switching of an external parameter λ, a so-called quantum quench, beyond a critical value λ_c the decay of the equilibrium order parameter has been found to show an abrupt change from monotonic to oscillatory. Surprisingly, the critical value λ_c in some cases coincides with the location of the respective equilibrium critical point[3,11,12].

The aim of this work is to link this sharp appearance of the order parameter oscillations to a recently introduced concept of a dynamical quantum phase transition (DQPT)[12]. In equilibrium, phase transitions are associated with nonanalyticities in partition functions or the respective thermodynamic potentials as a function of the control parameter. In Ref.[12] it has been shown that the nonequilibrium real-time evolution after a quantum quench can generate nonanalyticities as a function of time in Loschmidt amplitudes

$$G(t) = \langle\psi_0|e^{-iHt}|\psi_0\rangle, \tag{1}$$

where $|\psi_0\rangle$ is the initial state (typically the ground state of a Hamiltonian H_0 at λ_0) and H the Hamiltonian at the final value λ of the switched parameter. In the meantime DQPTs at critical times have been found in a variety of different systems[12,16–21]. Moreover, it has been shown numerically that these transitions are stable against weak perturbations that preserve the symmetries of the model[17]. It is important to emphasize that dynamical transitions have also been found in different contexts[22–25].

In equilibrium microscopic probabilities are directly related to measureable macroscopic quantities through the connection between partition functions and the thermodynamic potentials. Out of equilibrium there is a priori no direct link between the nonequilibrium microscopic probabilities or amplitudes, i.e., $G(t)$, and local observables which are the quantities that one is interested in from an experimental perspective. For quantum quenches in Ising and XY chains, however, there is numerical evidence[11,12,21] for such a connection although the underlying mechanism is still unclear.

It is the aim of this work to develop a theory linking DQPTs to the order parameter dynamics. It will be shown that this link is provided by a dynamical analogue to equilibrium critical regions connecting the properties of the system at zero energy to local observables at nonzero energies.

XXZ chain:- This connection will be studied for anisotropy quenches in the XXZ chain:

$$H_\Delta = J\sum_{l=0}^{N-1}\left[S_l^xS_{l+1}^x + S_l^yS_{l+1}^y + \Delta S_l^zS_{l+1}^z\right], \tag{2}$$

with $J>0$ antiferromagnetic, N the number of lattice sites, and S_l^α, $\alpha = x,y,x$, spin-1/2 operators. In equilibrium this model exhibits a quantum critical point at $\Delta = 1$ separating a gapless metallic phase ($\Delta<1$) from a gapped phase ($\Delta>1$) with antiferromagnetic order. The order parameter of this transition is the staggered magnetization

$$\mathcal{M}_s = \frac{1}{N}\sum_{l=0}^{N-1}(-1)^l S_l^z. \tag{3}$$

Nonequilibrium dynamics will be generated via a quantum quench[26]. The system is initialized in a Neél state:

$$|\psi_0\rangle = |\uparrow\downarrow\rangle = |\uparrow\downarrow\uparrow\downarrow\ldots\rangle, \tag{4}$$

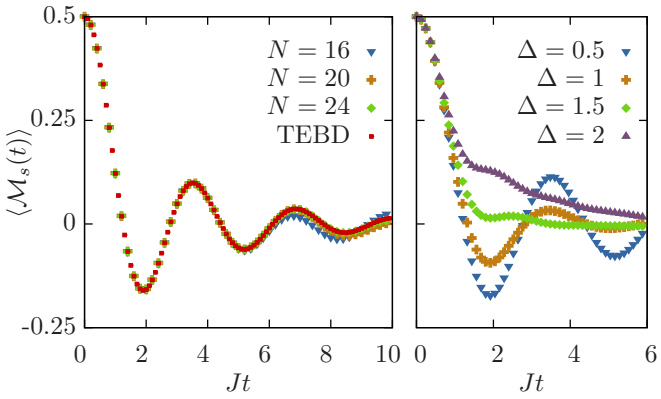

Figure 1: (color online) (a) Oscillatory decay of the staggered magnetization in the XXZ chain for initial Neél states and final anisotropies $\Delta = 0.6$ obtained using exact diagonalization (ED) for different system sizes N. Up to times $Jt = 10$ shown in this plot the ED data for $N = 24$ matches the thermodynamic limit result from TEBD obtained using the ALPS libraries[28]. (b) Increasing the anisotropy from $\Delta = 0.5$ to $\Delta = 2$ (for $N = 24$) the decay of the staggered magnetization changes from oscillatory to monotonic, see also Ref.[3].

which is equivalent to preparing the system in the ground state of the XXZ chain at initial anisotropy $\Delta_0 \to \infty$. The quantum real-time evolution is driven by the final Hamiltonian $H = H_\Delta$ at anisotropy $\Delta < \infty$. The numerical results are obtained using exact diagonalization (ED) based on a Lanczos tridiagonalization of the Hamiltonian with full reorthogonalization[27]. For the numerical calculations periodic boundary conditions have been chosen.

For initial Neél states the staggered magnetization shows a transition from a monotonic long-time decay to oscillatory as soon as $\Delta < 1$ crosses the equilibrium phase boundary[3,7]. Within some intermediate regime $1 < \Delta \lesssim 2$ the long-time behavior is monotonic, on transient time scales, however, oscillatory behavior can be found. In Fig. 1 ED data illustrates the oscillatory decay for quenches to a final $\Delta = 0.6$ and the transition to monotonic decay by increasing the anisotropy. Moreover, analytical and numerical results show that the model also exhibits real-time nonanalyticities in Loschmidt amplitudes and thus DQPTs[18,19].

Spectral decomposition:- At $\Delta_0 \to \infty$ the staggered magnetization $\mathcal{M}_s$ and the initial Hamiltonian H_{Δ_0} commute such that both observables can be measured simultaneously. It is therefore possible to decompose the staggered magnetization spectrally during its dynamical evolution:

$$\langle \mathcal{M}_s(t) \rangle = \int d\varepsilon \; \mathcal{M}_s(\varepsilon, t) \; P(\varepsilon, t). \tag{5}$$

Here, $P(\varepsilon, t)$ is the probability distribution that the system has energy density ε at time t (with energies measured by H_{Δ_0}) and $\mathcal{M}_s(\varepsilon, t)$ is the contribution to the full expectation value $\langle \mathcal{M}_s(t) \rangle$ from energy density ε weighted by $P(\varepsilon, t)$. The energy density distribution $P(\varepsilon, t)$ is defined by

$$P(\varepsilon, t) = \sum_\nu |\langle E_\nu | \psi_0(t) \rangle|^2 \delta(E_\nu / N - \varepsilon), \tag{6}$$

with $|\psi_0(t)\rangle = e^{-iHt}|\psi_0\rangle$ the time evolved initial state and $|E_\nu\rangle$ a complete set of eigenstates of the initial Hamiltonian H_{Δ_0} with the respective energies E_ν. For technical details, see below. The zero of energy is chosen such that the ground state of H_{Δ_0} has vanishing energy.

It is important to emphasize that in the context of Eq. (5) energies are *not* measured with the final Hamiltonian but rather with the initial one. Thereby, an "exclusive" perspective[29] is chosen in the sense that the perturbation which generates the nonequilibrium dynamics is not included into the system's internal energy. This choice is based on the observation that all properties addressed in the present work, the staggered magnetization as the order parameter for the antiferromagnetic phase and the Loschmidt amplitude as a ground state to ground state overlap, are rather connected to the initial than the final Hamiltonian.

Dynamical phase transitions:- In the following, it will be shown that $P(\varepsilon \to 0, t) = \mathcal{L}(t)$ is a Loschmidt echo $\mathcal{L} = |G(t)|^2$ and as such inherits the DQPT. Most importantly, dynamical transitions in $P(0, t)$ directly result in real-time nonanalyticities of $\mathcal{M}_s(0, t)$. These zero energy transitions in $\mathcal{M}_s(0, t)$ although smoothed extend their influence to nonzero energies $\mathcal{M}_s(\varepsilon > 0, t)$ leading to an oscillatory decay of the full expectation value $\langle \mathcal{M}_s(t) \rangle$. This connection directly generalizes to other systems with symmetry-broken phases.

Due to the twofold degeneracy of the ground state manifold in $\mathbb{Z}_2$ symmetry-broken phases the zero energy density $\varepsilon \to 0$ limit of the energy distribution contains two contributions which in the present XXZ chain are

$$P(0, t) = \mathcal{L}_{\uparrow\downarrow}(t) + \mathcal{L}_{\downarrow\uparrow}(t), \tag{7}$$

with $\mathcal{L}_\eta(t) = |\langle \eta | \psi_0(t) \rangle|^2$ and $\eta = \uparrow\downarrow, \downarrow\uparrow$ labeling the two degenerate ground states of H_{Δ_0}. For large systems $N \gg 1$ each of the microscopic probabilities $\mathcal{L}_\eta(t)$ obeys a large deviation scaling[30] $\mathcal{L}_\eta(t) = \exp[-N\lambda_\eta(t)]$ where the rate functions $\lambda_\eta(t)$ are intensive[12]. As a consequence, one of the two overlaps will always dominate:

$$P(0, t) = e^{-N\lambda(t)}, \;\; \lambda(t) = \min_\eta \lambda_\eta(t), \tag{8}$$

up to exponentially small corrections. In Fig. 2 plots of the rate functions $\lambda_\eta(t)$ are shown at $\Delta = 0.6$ for different system sizes N. At each N the two rate functions $\lambda_\eta(t)$ cross at a time $t^*(N)$ yielding a kink in $\lambda(t)$ due to the sudden switching between the two symmetry-broken sectors. The location of the intersection point in the thermodynamic limit can be found by finite-size scaling which yields $t^* \approx 1.40/J$, see Fig. 2. In the context of its definition according to Ref.[12] the system exhibts a *dynamical* quantum phase transition at t^*. It is important to emphasize that in this way it is possible to detect a DQPT

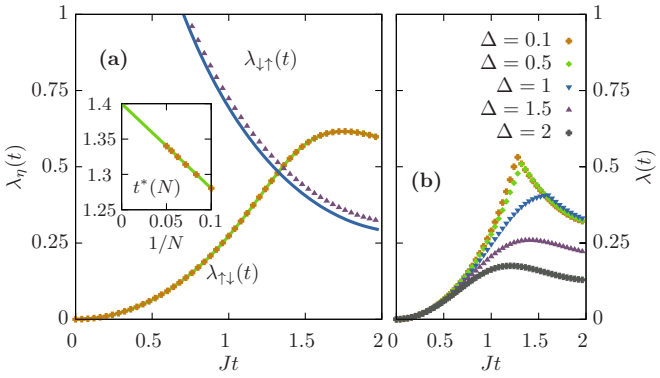

Figure 2: (color online) Dynamical quantum phase transition (DQPT) from ED. (a) The two overlap rate functions $\lambda_\eta(t)$ with $\eta = \uparrow\downarrow, \downarrow\uparrow$, each for two different system sizes $N = 16$ (lines) and $N = 24$ (dots) at anisotropy $\Delta = 0.6$. At each N the $\lambda_\eta(t)$ cross each other indicating a DQPT in $\lambda(t) = \min_\eta \lambda_\eta(t)$. While the $\lambda_{\uparrow\downarrow}(t)$ component shows no appreciable finite-size scaling, the curve of $\lambda_{\downarrow\uparrow}(t)$ shifts to larger times for increasing N. The location of the DQPT in the thermodynamic limit can be estimated by studying the system size dependence of the intersection point $t^*(N)$ of $\lambda_{\uparrow\downarrow}(t)$ and $\lambda_{\downarrow\uparrow}(t)$, see inset. A fit to data gives a DQPT at $t^* \approx 1.40/J$. In (b) the behavior of $\lambda(t)$ is shown for different anisotropies Δ at $N = 24$ indicating that for increasing Δ the DQPT is shifted to larger times eventually moving beyond $Jt = 2$. For times $Jt > 2$ (not shown) finite-size effects in the overlaps, but not the staggered magnetization, see Fig. 1, become substantial preventing a detailed analysis in this regime.

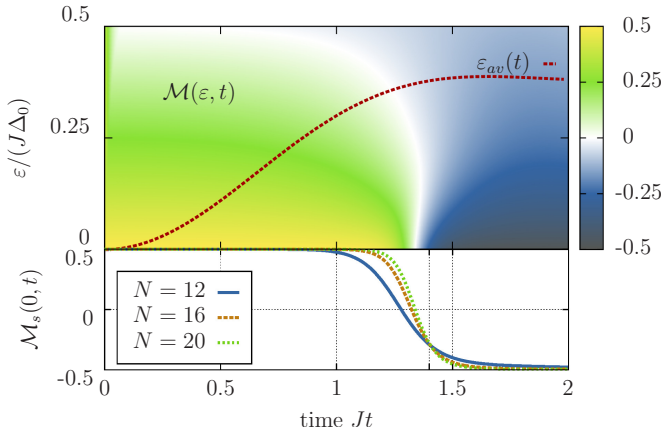

Figure 3: (color online) Upper false-color plot: Energy-resolved staggered magnetization $\mathcal{M}_s(\varepsilon, t)$ in the $\varepsilon - t$ plane for quenches to a final anisotropy $\Delta = 0.6$ and for a system of size $N = 20$. The DQPT at $\varepsilon = 0$ gets smeared at nonzero energies but its influence, a change in sign of the staggered magnetization, extends to $\varepsilon > 0$. The dominant contribution to $\langle \mathcal{M}_s(t) \rangle$ comes from a narrow interval in the vicinity of $\varepsilon = \varepsilon_{\rm av}(t)$, see main text, the dotted line depicts its dynamics. Lower plot: Zero-energy limit $\mathcal{M}_s(0, t)$ for different system sizes N. For increasing N the change in staggered magnetization becomes sharper eventually yielding a jump as one can directly infer from Fig. 2. As in Fig. 2 one can see that the point $t^*(N)$ where $\mathcal{M}_s(0, t)$ becomes zero (where $\lambda_{\uparrow\downarrow}(t) = \lambda_{\downarrow\uparrow}(t)$) shifts to larger times for larger N. A close inspection shows that there is a point $t \approx 1.40/J$ in time (indicated by a dashed line) where $\mathcal{M}_s(0, t)$ for all N considered intersect each other which yields the location of the DQPT as already estimated in Fig. 2.

occurring only in the thermodynamic limit[12] from finite-size ED data with high accuracy. Notice that $P(0, t)$ does not suffer from an ambiguity concerning the choice of the state $|\psi_0\rangle$ for the Loschmidt amplitude $G(t)$ in Eq. (1) in case of a ground state degeneracy. Due to the large deviation scaling of both $\mathcal{L}_\eta(t)$ with $\eta = \uparrow\downarrow, \downarrow\uparrow$ one obtains that $P(0, t) = |G(t)|^2$ for any choice of $|\psi_0\rangle = a|\uparrow\downarrow\rangle + b|\downarrow\uparrow\rangle$ within the ground state manifold as long as $|a|, |b| \neq 0$ and $N \gg 1$. In recent analytical and numerical work[18,19] it has been shown that for $\Delta > 1$, but not too large, DQPTs can exist which are, however, not connected to the switching between the two symmetry-broken sectors but rather occur in $\lambda_\eta(t)$ directly[19]. In analogy to nonanalyticities in $\lambda(t)$ as a switching between two symmetry-broken sectors this may hint towards a different internal structure in $\lambda_\eta(t)$ in these cases.

Energy-resolved staggered magnetization:- As $\mathcal{M}_s$ and H_{Δ_0} commute at $\Delta_0 \to \infty$ both observables can be measured simultaneously such that

$$\langle \mathcal{M}_s(t) \rangle = \int d\varepsilon \int dm \; m \, P(\varepsilon, m; t), \tag{9}$$

with $P(\varepsilon, m; t)$ the joint distribution function that the system has energy density ε and staggered magnetization density m at time t. Eq. (9) reflects the potential to perform the following measurement sequence: first a projective energy measurement onto the eigenstate $|E\rangle$ with energy density $\varepsilon = E/N$ followed by a measurement of the staggered magnetization.

In the large system size limit $N \gg 1$ the distribution $P(\varepsilon, m; t)$ obeys a large-deviation scaling[30] $P(\varepsilon, m; t) = \exp[-N\theta(\varepsilon, m; t)]$ with $\theta(\varepsilon, m; t)$ an intensive function, see App. A. As a consequence, $P(\varepsilon, m; t)$ satisfies a central-limit theorem[30] such that at a given ε only a narrow region (vanishingly small in the thermodynamic limit) contributes dominantly in the vicinity of $m = m^*(\varepsilon, t)$ with $m^*(\varepsilon, t)$ given by $\inf_m \theta(\varepsilon, m; t)$. This yields the desired result in Eq. (5) with the identification $\mathcal{M}_s(\varepsilon, t) = m^*(\varepsilon, t)$ and $P(\varepsilon, t) = P(\varepsilon, m^*(\varepsilon, t); t)$. Using large-deviation theory it is straightforward to compute $\mathcal{M}_s(\varepsilon, t)$ as the expectation value $\mathcal{M}_s(\varepsilon, t) = \langle \psi_0(t, s)|\mathcal{M}_s|\psi_0(t, s)\rangle$ in the state $|\psi_0(t, s)\rangle = [\mathcal{N}(s, t)]^{-1/2} e^{-H_{\Delta_0} s/2}|\psi_0(t)\rangle$ with $\mathcal{N}(s, t) = \langle \psi_0(t)|e^{-H_{\Delta_0} s}|\psi_0(t)\rangle$ and $s = s(\varepsilon, t)$ given by the solution of the equation $\varepsilon = N^{-1}\langle \psi_0(t, s)|H_{\Delta_0}|\psi_0(t, s)\rangle$, see App. A. Notice that these results become asymptotically exact in the thermodynamic limit such that the finite-size systems studied with ED may contain corrections that only vanish for $N \to \infty$.

In Fig. 3 a false-color plot of $\mathcal{M}_s(\varepsilon, t)$ obtained via ED is shown in the $\varepsilon - t$ plane. Additionally, a finite-size scaling of the staggered magnetization at zero energy is

included revealing for times $t < t^*$ that $\mathcal{M}_s(0,t) \to 1/2$ whereas for $t > t^*$ that $\mathcal{M}_s(0,t) \to -1/2$. At $t \approx t^*$ there is a crossover which becomes sharper for increasing system sizes. In the thermodynamic limit this yields a jump because from Fig. (2) one can directly infer that at $t = t_*$ the dominant contribution in the zero energy sector switches from $\eta = \uparrow\downarrow$ with staggered magnetization $+1/2$ to $\eta = \downarrow\uparrow$ with staggered magnetization $-1/2$. Thus, the DQPT in the Loschmidt amplitude directly translates into a real-time nonanalyticity in the zero-energy limit $\mathcal{M}_s(0,t)$ of the order parameter.

How does this nonanalyticity at zero energy influence the dynamics of the full expectation value $\langle \mathcal{M}_s(t) \rangle$ of the staggered magnetization? In the thermodynamic limit the dominant contribution to $\langle \mathcal{M}_s(t) \rangle$ comes from a narrow interval in the vicinity of $\varepsilon = \varepsilon_{\rm av}(t) = N^{-1} \langle H_0(t) \rangle$ due to the central limit theorem such that $\langle \mathcal{M}_s(t) \rangle \to \mathcal{M}_s(\varepsilon_{\rm av}(t), t)$ for $N \to \infty$. In order to assess the influence of the DQPT onto $\langle \mathcal{M}_s(t) \rangle$ it is therefore necessary to study potential connections between $\mathcal{M}_s(0,t)$ and $\mathcal{M}_s(\varepsilon_{\rm av}(t), t)$.

As one can see from Fig. 3, the real-time nonanalyticity gets smeared at nonzero energies. Its influence, however, extends to $\varepsilon > 0$ as a matter of continuity: the change in sign of $\mathcal{M}_s(\varepsilon > 0, t)$ is not abrupt any more, but spans over a time interval of nonzero length. The larger the energy density the larger the region in the $\varepsilon - t$ plane which is controlled by the zero-energy real-time nonanalyticity. This extends up to energy densities $\varepsilon_{\rm av}(t)$ demonstrating that DQPTs control the sign change of the order parameter and as a consequence its oscillatory decay. Notice the strong similarity to critical regions at equilibrium quantum phase transitions by associating energy density with temperature and time with the control parameter.

The energy-resolved staggered magnetization $\mathcal{M}_s(\varepsilon, t)$ can, in principle, be measured using postselection[12], the limit of zero energy density where the DQPT occurs, however, will hardly be accessible. This is in complete analogy to equilibrium where the limit of zero temperature can never be reached prohibiting direct access to zero-temperature quantum phase transitions, for example. But still there exist quantum critical regions in the phase diagram at nonzero temperature where nonanalyticities are smeared, the presence of the nearby quantum critical point, however, still dominates the physical properties. In complete analogy, in the present nonequilibrium scenario one can see that the influence of the DQPT at zero energy extends up to nonzero energies at times near t^* such that the DQPT controls the macroscopic properties in this regime by inducing a sign change of the staggered magnetization in Fig. 1. As a consequence, the oscillatory decay of the order parameter $\langle \mathcal{M}_s(t) \rangle$ is intimately connected to underlying DQPTs in Loschmidt echos via a nonequilibrium analogue to critical regions.

It is important to emphasize that, although there is an apparent similarity between Fig. 3 and equilibrium critical regions, it is not clear whether universality and scaling apply for the DQPT in the XXZ chain studied here. On the one hand, the DQPT due to a switching between the two symmetry-broken sectors is reminiscent to first-order ground state phase transitions in consequence of a level crossing. On the other hand, jumps in derivatives of thermodynamic potentials can also appear for continuous phase transitions such as in the specific heat of the superconducting-normal state transition in BCS theory. Adressing these general questions of scaling and universality as well as a potential classification scheme for the DQPTs requires some further detailed analysis which is left open for future work.

The results obtained here for the XXZ chain naturally generalize to other models as long as the following two requirements are satisfied: firstly, the initial Hamiltonian has to exhibit a ground-state degeneracy such that $P(0,t)$ is a sum over the individual probabilities to be in the one of the respective ground states, see Eq. (7). Secondly, the initial Hamiltonian has to exhibit one point in parameter space where it commutes with the order parameter allowing for the spectral decomposition in Eq. (5). One case satisfying these requirements is the transverse-field Ising chain with vanishing initial magnetic field, for example.

The connection between DQPTs and macroscopic dynamical properties is a priori not limited to the order parameter alone. For any observable whose expectation value differs in the two symmetry-broken ground states DQPTs in Loschmidt echos impose real-time nonanalyticities in the ground-state manifold as for the zero-energy limit of the order parameter, see Fig. 3.

The scenario studied in this work is restricted to a specific initial condition $\Delta_0 \to \infty$. An important question therefore is the extension to the more general case $\Delta_0 < \infty$. Although order parameter and initial Hamiltonian do not commute any more, the respective eigenstates and eigenvalues depend smoothly on Δ_0 as long as Δ_0 does not cross the equilibrium critical point suggesting that the overall picture presented here for a particular case remains still valid.

Conclusions:- In this work it has been shown that the order parameter dynamics in the XXZ chain from initial Neél states is directly connected to underlying dynamical quantum phase transitions in Loschmidt echos. The dynamical quantum phase transitions can be associated with a switching between the two symmetry-broken sectors in the twofold degenerate ground state manifold. Based on a spectral decomposition of the staggered magnetization, see Eq. (5), it has been shown that this directly leads to a real-time nonanalyticity in the zero-energy limit of the order parameter dynamics. At nonzero energies this nonanalyticity is smeared but there exists a region in the $\varepsilon - t$ plane whose properties are controlled by the zero-energy phase transition, see Fig. 3. As a consequence, the decay of the staggered magnetization exhibits a nonmonotonic oscillatory behavior. These results generalize also to other observables and to other systems hosting symmetry-broken phases.

Acknowledgments

Valuable discussions with Philipp Hauke, Anatoli Polkovnikov, and Stefan Kehrein are gratefully acknowledged. This work has been supported by the Deutsche Akademie der Naturforscher Leopoldina via the grant LPDS 2013-07 and by the Austrian Science Fund FWF (SFB FOQUS F4016). The exact diagonalization algorithm uses the Armadillo linear algebra libraries[31].

[1] R. A. Barankov and L. S. Levitov, Phys. Rev. Lett. **96**, 230403 (2006).
[2] E. A. Yuzbashyan and M. Dzero, Phys. Rev. Lett. **96**, 230404 (2006).
[3] P. Barmettler, M. Punk, V. Gritsev, E. Demler, and E. Altman, Phys. Rev. Lett. **102**, 130603 (2009).
[4] M. Eckstein, M. Kollar, and P. Werner, Phys. Rev. Lett. **103**, 056403 (2009).
[5] M. Eckstein, M. Kollar, and P. Werner, Phys. Rev. B **81**, 115131 (2010).
[6] M. Schiro and M. Fabrizio, Phys. Rev. Lett. **105**, 076401 (2010).
[7] P. Barmettler, M. Punk, V. Gritsev, E. Demler, and E. Altman, New Journal of Physics **12**, 055017 (2010).
[8] A. Gambassi and P. Calabrese, Eur. Phys. Lett. **95**, 66007 (2011).
[9] M. Schiro and M. Fabrizio, Phys. Rev. B **83**, 165105 (2011).
[10] L. Mathey, K. L. Günter, J. Dalibard, and A. Polkovnikov, arXiv (2011).
[11] P. Calabrese, F. H. L. Essler, and M. Fagotti, J. Stat. Mech. p. P07016 (2012).
[12] M. Heyl, A. Polkovnikov, and S. Kehrein, Phys. Rev. Lett. **110**, 135704 (2013).
[13] B. Sciolla and G. Biroli, Phys. Rev. Lett. **105**, 220401 (2010).
[14] B. Sciolla and G. Biroli, J. Stat. Mech. P11003 (2011).
[15] F. Igloi and G. Roosz, New Journal of Physics **15**, 023036 (2013).
[16] F. Pollmann, S. Mukerjee, A. G. Green, and J. E. Moore, Phys. Rev. E **81**, 020101(R) (2010).
[17] C. Karrasch and D. Schuricht, Phys. Rev. B **87**, 195104 (2013).
[18] M. Fagotti, arXiv p. 1308.02777 (2013).
[19] F. Andraschko and J. Sirker, arXiv p. 1312.4165 (2013).
[20] J. M. Hickey, S. Genway, and J. P. Garrahan, Phys. Rev. B **89**, 054301 (2014).
[21] S. Vajna and B. Dora, arXiv p. 1401.2865 (2014).
[22] L. O. Hedges, R. L. Jack, J. P. Garrahan, and D. Chandler, Science **323**, 1309 (2009).
[23] J. P. Garrahan and I. Lesanovsky, Phys. Rev. Lett. **104**, 160601 (2010).
[24] S. Diehl, A. Tomadin, A. Micheli, R. Fazio, and P. Zoller, Phys. Rev. Lett. **105**, 015702 (2010).
[25] A. Mitra, Phys. Rev. Lett. **109**, 260601 (2012).
[26] A. Polkovnikov, K. Sengupta, A. Silva, and M. Vengalattore, Rev. Mod. Phys. **83**, 863 (2011).
[27] J. K. Cullum and R. A. Willoughby, *Lanczos Algorithms for Large Symmetric Eigenvalue Computations* (Society for Industrial and Applied Mathematics, Philadelphia, 2002).
[28] B. Bauer, L. D. Carr, H. G. Evertz, A. E. Feiguin, J. Freire, S. Fuchs, L. Gamper, J. Gukelberger, E. Gull, S. Guertler, et al., J. Stat. Mech. p. P05001 (2011).
[29] M. Campisi, P. Talkner, and P. Hänggi, Philos. Transact. A Math. Phys. Eng. Sci. **369**, 291 (2011).
[30] H. Touchette, Phys. Rep. **478**, 1 (2009).
[31] C. Sanderson, Technical report, Nicta (2010).

Appendix A: Spectral decomposition of the staggered magnetization and large deviation theory

The aim of this appendix is to outline the calculation of the joint probability distribution function $P(\varepsilon, m; t)$ that the system at time t has energy density ε and staggered magnetization m using large deviation theory[30]. This then directly leads to a computational scheme for the calculation of the energy-resolved staggered magnetization $\mathcal{M}_s(\varepsilon, t)$.

The joint probability distribution $P(\varepsilon, m; t)$ is defined as:

$$P(\varepsilon, m; t) = \sum_\nu |\langle E_v|\psi_0(t)\rangle|^2 \delta(\varepsilon - e_\nu)\delta(m_\nu - m) \quad \text{(A1)}$$

where $e_\nu = E_\nu/N$ is the energy density and m_ν is the staggered magnetization of the state $|E_\nu\rangle$: $H_{\Delta_0}|E_\nu\rangle = Ne_\nu|E_\nu\rangle$ and $\mathcal{M}_s|E_\nu\rangle = m_\nu|E_\nu\rangle$. The function

$$\begin{aligned} G(s, \mu; t) &= \sum_\nu |\langle E_v|\psi_0(t)\rangle|^2 e^{-sE_\nu} e^{-\mu N m_\nu} \\ &= \langle\psi_0(t)|e^{-sH_{\Delta_0}} e^{-\mu N \mathcal{M}_s}|\psi_0(t)\rangle \end{aligned} \quad \text{(A2)}$$

is related to $P(\varepsilon, m; t)$ via

$$G(s, \mu; t) = \int d\varepsilon \int dm P(\varepsilon, m; t) e^{-N\varepsilon s} e^{-Nm\mu}. \quad \text{(A3)}$$

The generating function $G(s, \mu; t)$ obeys a large-deviation scaling[12]:

$$G = e^{N g(s,\mu;t)} \quad \text{(A4)}$$

with $g(s, \mu; t)$ an intensive function independent of system size N. As a consequence of this large deviation scaling the joint distribution function has to be of the following structure[30]

$$P(\varepsilon, m; t) = e^{-N\theta(\varepsilon,m;t)} \quad \text{(A5)}$$

with the rate function $\theta(\varepsilon, m; t)$ again intensive and given by the following series of Legendre transforms:

$$\begin{aligned} \theta(\varepsilon, m; t) &= -\inf_\mu \left[\mu m + \varphi(\varepsilon, \mu; t)\right], \\ \varphi(\varepsilon, \mu; t) &= \inf_s \left[\varepsilon s + g(s, \mu; t)\right]. \end{aligned} \quad \text{(A6)}$$

The corresponding back transformations read:

$$\varphi(\varepsilon,\mu;t) = -\inf_m \left[\mu m + \theta(\varepsilon,m;t)\right],$$
$$g(s,\mu;t) = -\inf_\varepsilon \left[\varepsilon s - \varphi(\varepsilon,\mu;t)\right]. \tag{A7}$$

As in thermodynamics the Legendre transform of $\theta(\varepsilon,m;t)$, for example, can be calculated by:

$$\varphi(\varepsilon,\mu;t) = -\mu m(\varepsilon,\mu;t) - \theta(\varepsilon,m(\varepsilon,\mu;t);t) \tag{A8}$$

with $m(\varepsilon,\mu;t)$ solving the "equation of state":

$$\mu = -\frac{d\theta(\varepsilon,m;t)}{dm}. \tag{A9}$$

In order to obtain the energy-resolved staggered magnetization $\mathcal{M}_s(\varepsilon,t)$ it is necessary to determine the infimum of $\theta(\varepsilon,m;t)$ over all m which according to the previous formulas is

$$\varphi(\varepsilon,0;t) = -\inf_m \left[\theta(\varepsilon,m;t)\right]. \tag{A10}$$

Thus, the infimum happens at $\mu = 0$ such that from the equation of state

$$m^*(\varepsilon,t) = -\left.\frac{\partial\varphi(\varepsilon,\mu;t)}{\partial\mu}\right|_{\mu=0} = -\left.\frac{\partial g}{\partial\mu}\right|_{s=s(\varepsilon,\mu;t),\mu=0}$$
$$= \langle\psi_0(t,s)|\mathcal{M}_s(t)|\psi_0(t,s)\rangle|_{s=s(\varepsilon,\mu=0;t)}, \tag{A11}$$

with

$$|\psi_0(t,s)\rangle = \frac{e^{-sH_{\Delta_0}/2}}{\sqrt{\mathcal{N}}}|\psi_0(t)\rangle,$$
$$\mathcal{N} = \langle\psi_0(t)|e^{-sH_{\Delta_0}}|\psi_0(t)\rangle, \tag{A12}$$

and $s = s(\varepsilon,\mu=0,t)$ solves the equation of state

$$\varepsilon = \frac{1}{N}\langle\psi_0(t,s)|H_{\Delta_0}|\psi_0(t,s)\rangle. \tag{A13}$$

This yields the formulas presented in the main text.